

## Reaction cross sections of hypernuclei and the shrinkage effect

T. Akaishi and K. Hagino

*Department of Physics, Tohoku University, Sendai 980-8578, Japan*

(Received 11 September 2013; published 25 October 2013)

We calculate the reaction cross sections for  ${}^6\text{Li}$  and  ${}^7_\Lambda\text{Li}$  on a  ${}^{12}\text{C}$  target at 100 MeV/nucleon using the Glauber theory. To this end, we assume a two-body cluster structure for  ${}^6\text{Li}$  and  ${}^7_\Lambda\text{Li}$ , and employ the few-body treatment of the Glauber theory, that is beyond the well known optical limit approximation. We show that the reaction cross section for  ${}^7_\Lambda\text{Li}$  is smaller than that for  ${}^6\text{Li}$  by about 4%, reflecting the shrinkage effect of the  $\Lambda$  particle.

DOI: [10.1103/PhysRevC.88.047603](https://doi.org/10.1103/PhysRevC.88.047603)

PACS number(s): 21.80.+a, 25.60.Dz, 21.10.Gv, 27.20.+n

One of the main interests in hypernuclear physics is the change of the nuclear structure due to a few  $\Lambda$  particles, which is referred to as the impurity effect [1–16]. A  $\Lambda$  particle can enter the interior of a nucleus since it does not receive the Pauli exclusion principle from nucleons, and attracts the surrounding nucleons. Various theoretical analyses and experimental measurements have suggested that this effect appears as a shrinkage of a nucleus, that is, the change of the nuclear size [1–6]. Particularly, a large shrinkage effect is expected for light nuclei which have cluster structures [1–3], since clusters are in general weakly bound in these nuclei. The shrinkage of hypernuclei has been investigated experimentally with  $\gamma$ -ray spectroscopy [4,5]. In the experiment of Ref. [5], the electric quadrupole transition probability  $B(E2)$  from the excited  $5/2^+$  state to the ground state in  ${}^7_\Lambda\text{Li}$  was measured. The observed  $B(E2)$  value of  ${}^7_\Lambda\text{Li}$  was smaller than that of  ${}^6\text{Li}$  by about 33%. This corresponds to about 19% shrinkage of the intercluster distance if one assumes the two-body cluster structure with core+deuteron (that is,  $\alpha + d$  and  ${}^5_\Lambda\text{He} + d$  for  ${}^6\text{Li}$  and  ${}^7_\Lambda\text{Li}$ , respectively) [5].

In this paper, we investigate the shrinkage effect of the  $\Lambda$  particle using reaction cross sections with the Glauber theory. The reaction cross section is defined as a sum of all cross sections except for the elastic scattering, and it has played an important role in the discussion of a density distribution for neutron-rich nuclei, such as a “halo” structure of exotic nuclei [17–21]. Classically, if a projectile and a target nuclei are assumed to be spheres with radii of  $R_P$  and  $R_T$ , respectively, the reaction cross section  $\sigma_R$  is given as  $\sigma_R = \pi(R_P + R_T)^2$ . The experimental cross sections have indeed shown that the reaction cross section increases for nuclei which have a halo structure,<sup>1</sup> and the reaction cross sections have thus been used as a standard tool to extract the nuclear size of neutron-rich nuclei [18]. It is thus intriguing to study the reaction cross sections of hypernuclei and discuss their size.

In order to extract the nuclear size and matter distributions, the Glauber theory [22] has often been used [23–26]. Notice

<sup>1</sup>Experimentally, the interaction cross sections, defined as a sum of cross sections in which the nucleon number changes, are actually measured instead of the reaction cross sections at intermediate and high energies. At these energies the interaction and the reaction cross sections do not differ much, especially for weakly bound systems, because inelastic scattering cross sections are small.

that the Glauber-type analyses need only the ground state information. This makes our study complementary to the method with electromagnetic transitions, which involves both the ground and excited states.

We choose  ${}^6\text{Li}$  and  ${}^7_\Lambda\text{Li}$  nuclei as projectiles and  ${}^{12}\text{C}$  as a target. Since these projectile nuclei are known to have a two-body cluster structure [6,27], we adopt the semimicroscopic cluster model [27,28] in order to obtain the ground state wave functions. In this model, the intercluster potentials between the core and deuteron are constructed based on the core +  $p$  +  $n$  structure. For the  $s$ -wave state (that is, the ground state), it is given as

$$V(R) = \int d\mathbf{r} [V_{\text{cN}}(\mathbf{R} + \mathbf{r}/2) + V_{\text{cN}}(\mathbf{R} - \mathbf{r}/2)] \cdot |\psi_d(\mathbf{r})|^2, \quad (1)$$

where  $\psi_d(\mathbf{r})$  is an  $s$ -state wave function for the relative motion between the proton and the neutron in the deuteron cluster.  $V_{\text{cN}}$  is the potential between the nucleons and the core nucleus. In our calculations, we employ an exponential form for the deuteron wave function [29]:  $\psi_d(r) = \sqrt{2\alpha}e^{-\alpha r}/\sqrt{4\pi r}$ ,  $\alpha = 0.2316 \text{ fm}^{-1}$ , and a Gaussian-type potential between the  $\alpha$  particle and the nucleon [6]:  $V_{\alpha\text{N}}(r) = -v_0e^{-\beta r^2}$ ,  $v_0 = 40.45 \text{ MeV}$ , and  $\beta = 0.189 \text{ fm}^{-2}$ . For  ${}^7_\Lambda\text{Li}$  nucleus, one also has to add the  $\Lambda$ -nucleon potential to  $V_{\text{cN}}$ , that is,  $V_{\text{cN}} = V_{\alpha\text{N}} + V_{\Lambda\text{N}}$ . In order to construct it, we fold a  $\Lambda$ -nucleon potential  $v_{\Lambda\text{N}}$  in the free space with the  $\Lambda$  particle density in the  $\alpha$  cluster,

$$V_{\Lambda\text{N}}(r) = \int d\mathbf{r}' \rho_\Lambda(\mathbf{r}') v_{\Lambda\text{N}}(\mathbf{r} - \mathbf{r}'). \quad (2)$$

For a Gaussian density distribution,  $\rho_\Lambda(r) = (\pi b_\Lambda^2)^{-2/3} e^{-r^2/b_\Lambda^2}$ , and a Gaussian  $\Lambda$ -nucleon potential,  $v_{\Lambda\text{N}}(r) = -v_0 e^{-r^2/b_v^2}$ , this can be calculated analytically as

$$V_{\Lambda\text{N}}(r) = -v_0 \left( \frac{b_v^2}{b_\Lambda^2 + b_v^2} \right)^{3/2} \exp \left[ -\frac{r^2}{b_\Lambda^2 + b_v^2} \right]. \quad (3)$$

We numerically solve the Schrödinger equation with the potential  $V(R)$ , Eq. (1). The ground state is identified as the state with the node of 1 [6,27]. In this paper, we use the same width and strength parameters,  $b_\Lambda$ ,  $b_v$ , and  $v_0$ , as those in Ref. [6].

Figure 1 shows the intercluster radial wave functions  $u(R)$  so obtained, where  $u(R)$  is defined with the intercluster wave

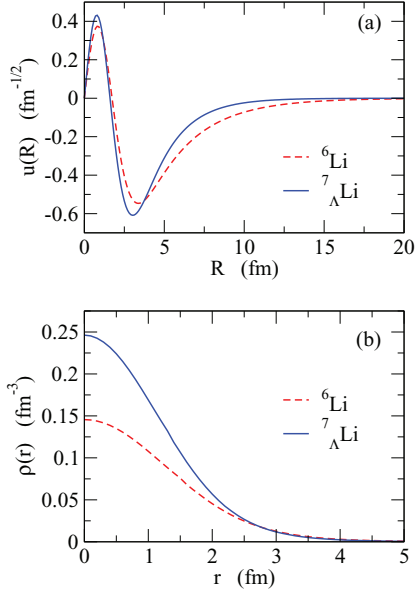


FIG. 1. (Color online) (a) The intercluster radial wave functions  $u(R)$ , defined as  $\psi_{\text{rel}}(\mathbf{R}) = \frac{u(R)}{R} Y_{00}(\hat{\mathbf{R}})$ , for the ground state of  ${}^6\text{Li}$  (the dashed line) and  ${}^7_{\Lambda}\text{Li}$  (the solid line) nuclei obtained with the semimicroscopic cluster model. The  $\alpha$  + deuteron and  ${}^5_{\Lambda}\text{He}$  + deuteron structures are assumed for  ${}^6\text{Li}$  and  ${}^7_{\Lambda}\text{Li}$ , respectively. (b) The same as (a), but for the one-body densities  $\rho(r)$  calculated with  $\psi_{\text{rel}}$ .

function  $\psi_{\text{rel}}(\mathbf{R})$  as  $\psi_{\text{rel}}(\mathbf{R}) = \frac{u(R)}{R} Y_{00}(\hat{\mathbf{R}})$ . The dashed and solid lines are for  ${}^6\text{Li}$  and  ${}^7_{\Lambda}\text{Li}$ , respectively. The figure also shows the one-body densities  $\rho(r)$  obtained as

$$\rho(\mathbf{r}) = \int d\mathbf{R} |\psi_{\text{rel}}(\mathbf{R})|^2 [\rho_1(\mathbf{r} + a_1 \mathbf{R}) + \rho_2(\mathbf{r} - a_2 \mathbf{R})], \quad (4)$$

where  $a_1$  and  $a_2$  are defined as  $M_2/(M_1 + M_2)$  and  $M_1/(M_1 + M_2)$ , respectively,  $M_1$  and  $M_2$  being the masses of clusters 1 and 2, respectively. We use Gaussian-type densities for  $d$  and  $\alpha$ ,  $\rho_i(r) = A_i (\pi \gamma_i^2)^{-2/3} e^{-r^2/\gamma_i^2}$ , where  $A_i$  is the mass number of the cluster  $i$  and  $\gamma_i = 1.36$  and  $1.60$  fm for  $i = \alpha$  and  $d$ , respectively, while the density for  ${}^5_{\Lambda}\text{He}$  is given by  $\rho_{\alpha} + \rho_{\Lambda}$ . One can see that the addition of the  $\Lambda$  particle shifts the wave function of  ${}^7_{\Lambda}\text{Li}$  towards smaller distances as compared to the wave function of  ${}^6\text{Li}$ . The root mean square (rms) radii for  ${}^6\text{Li}$  and  ${}^7_{\Lambda}\text{Li}$  are 4.342 and 3.527 fm, respectively. This amounts to a shrinkage of about 19%, which agrees well with the experimental data [5] as well as with more microscopic calculations in Refs. [1–3]. These densities and the wave functions are used in the Glauber calculations for reaction cross sections.

Let us now compute the reaction cross sections for the  ${}^6\text{Li} + {}^{12}\text{C}$  and  ${}^7_{\Lambda}\text{Li} + {}^{12}\text{C}$  systems at 100 MeV/nucleon with the Glauber theory. We first use the optical limit approximation (OLA) with a zero-range nucleon-nucleon interaction. The reaction cross section for  ${}^6\text{Li}$  in this approximation reads

$$\sigma_{\text{R}}^{\text{(OLA)}} = 2\pi \int b db [1 - e^{-\sigma_{\text{NN}} \int d\mathbf{s} \rho_p^{(z)}(-\mathbf{b} + \mathbf{s}) \rho_t^{(z)}(\mathbf{s})}], \quad (5)$$

where  $\sigma_{\text{NN}}$  is the total cross section for nucleon-nucleon scattering and  $b$  is an impact parameter.  $\rho^{(z)}$  is a  $z$ -integrated

density,  $\rho^{(z)}(s) \equiv \int dz \rho(\mathbf{r})$ , where  $s$  is the two-dimensional vector perpendicular to the beam axis, that is,  $\mathbf{r} = (s, z)$ . The reaction cross section for  ${}^7_{\Lambda}\text{Li}$  can also be obtained in a similar manner, by adding the contribution of the  $\Lambda$  particle in the exponent [see Eq. (9) below]. In our calculations, we use the Gaussian density distribution for  ${}^{12}\text{C}$  with the width parameter of  $\gamma_T = 1.89$  fm.

For comparison, we also compute the reaction cross sections using the few-body (FB) treatment [30] beyond the OLA, in order to take account of the cluster correlations in the projectiles (see also Ref. [31] for an alternative method which is beyond the OLA). The reaction cross sections in the FB are given as

$$\sigma_{\text{R}}^{\text{(FB)}} = 2\pi \int b db [1 - |\langle \psi_{\text{rel}} | S_1(b_1) S_2(b_2) | \psi_{\text{rel}} \rangle|^2], \quad (6)$$

where  $S_i(b_i)$  is the scattering matrix between the cluster  $i$  in the projectile and the target nuclei evaluated in the OLA. For  $d$  and  $\alpha$ ,  $S_i(b)$  is given by

$$S_i(b) = \exp \left[ -\frac{\sigma_{\text{NN}}}{2} \int d\mathbf{s} \rho_i^{(z)}(-\mathbf{b} + \mathbf{s}) \rho_T^{(z)}(\mathbf{s}) \right]. \quad (7)$$

Since we employ the Gaussian-type densities for all the clusters including the target, it can be obtained analytically as

$$S_i(b) = \exp \left[ -\frac{\sigma_{\text{NN}}}{2} \frac{A_i A_T}{\pi (\gamma_i^2 + \gamma_T^2)} e^{-b^2/(\gamma_i^2 + \gamma_T^2)} \right]. \quad (8)$$

For a hypernucleus  ${}^5_{\Lambda}\text{He}$ , Eq. (7) is extended as

$$S_{{}^5_{\Lambda}\text{He}}(b) = \exp \left[ -\frac{\sigma_{\text{NN}}}{2} \int d\mathbf{s} \rho_{\alpha}^{(z)}(-\mathbf{b} + \mathbf{s}) \rho_T^{(z)}(\mathbf{s}) - \frac{\sigma_{\Lambda\text{N}}}{2} \int d\mathbf{s} \rho_{\Lambda}^{(z)}(-\mathbf{b} + \mathbf{s}) \rho_T^{(z)}(\mathbf{s}) \right], \quad (9)$$

where  $\sigma_{\Lambda\text{N}}$  is the total cross section for  $\Lambda$ -nucleon scattering. We consider the energy region of  $E \simeq 100$  MeV/nucleon, where experimental cross sections for both  $\sigma_{\text{NN}}$  and  $\sigma_{\Lambda\text{N}}$  are available, although  $\sigma_{\Lambda\text{N}}$  has not been determined accurately. We take  $\sigma_{\text{NN}} = 55.2$  mb [32] and  $\sigma_{\Lambda\text{N}}$  in the range from 10 to 30 mb [33].

Table I shows the reaction cross sections obtained with the FB and the OLA calculations for  ${}^6\text{Li}$  and  ${}^7_{\Lambda}\text{Li}$ . We notice that

TABLE I. The reaction cross sections  $\sigma_{\text{R}}$ , in units of mb, for  ${}^6\text{Li}$  and  ${}^7_{\Lambda}\text{Li}$  incident on a  ${}^{12}\text{C}$  target at 100 MeV/nucleon. The values for the  $\Lambda$ -nucleon scattering cross section [33],  $\sigma_{\Lambda\text{N}}$ , in units of mb, are given in the parentheses. Both the results based on the few-body (FB) treatment and the optical limit approximation (OLA) for the Glauber theory are shown.

nucleus	FB	OLA
${}^6\text{Li}$	825.9	880.6
${}^7_{\Lambda}\text{Li}(\sigma_{\Lambda\text{N}} = 0)$	781.6	815.3
${}^7_{\Lambda}\text{Li}(\sigma_{\Lambda\text{N}} = 10)$	786.7	819.9
${}^7_{\Lambda}\text{Li}(\sigma_{\Lambda\text{N}} = 20)$	791.7	824.4
${}^7_{\Lambda}\text{Li}(\sigma_{\Lambda\text{N}} = 30)$	796.5	828.8

the OLA yields always larger reaction cross sections compared to the FB, indicating an importance of the cluster correlation in these nuclei. If one considers only the shrinkage of the nucleon distribution in  ${}^7_{\Lambda}\text{Li}$ , neglecting the contribution of the  $\Lambda$  particle to the reaction cross section (that is, setting  $\sigma_{\Lambda N} = 0$ ), the reaction cross section for  ${}^7_{\Lambda}\text{Li}$  decreases by about 5.4% in the FB and 7.4% in the OLA compared to the reaction cross section for  ${}^6\text{Li}$ . By including the  $\Lambda$  particle contribution to the reaction cross section, the reduction is in the range 4.7–3.6% in the FB and 6.9–5.9% in the OLA. Although these values are somewhat smaller than the reduction in the rms radius, these results clearly indicate that the shrinkage effect in hypernuclei can be studied also with the reaction cross section.

In summary, we have investigated reaction cross sections for  ${}^6\text{Li}$  and  ${}^7_{\Lambda}\text{Li}$  nuclei incident on a  ${}^{12}\text{C}$  target at 100 MeV/nucleon. We have first applied for these projectile

nuclei the semimicroscopic cluster model in order to construct the ground state wave functions and the one-body densities. For a reaction theory, we have used the FB treatment for the projectiles in the Glauber theory in order to take into account the cluster correlations. We have found that the reaction cross section for  ${}^7_{\Lambda}\text{Li}$  is always smaller than that for  ${}^6\text{Li}$  by about a few percent. This fact suggests that the shrinkage effect induced by a  $\Lambda$  particle in hypernuclei can be studied with reaction cross sections as an alternative to  $\gamma$ -ray spectroscopy. It would be interesting if a measurement of reaction cross sections could be realized for hypernuclei in the future.

We thank H. Tamura, Y. Tanimura, and Y. Urata for useful discussions. This work was supported by JSPS KAKENHI Grant No. 22540262.

- 
- [1] T. Motoba, H. Bandō, and K. Ikeda, *Prog. Theor. Phys.* **70**, 189 (1983).
- [2] T. Motoba, H. Bandō, K. Ikeda, and T. Yamada, *Suppl. Prog. Theor. Phys.* **81**, 42 (1985).
- [3] E. Hiyama, M. Kamimura, K. Miyazaki, and T. Motoba, *Phys. Rev. C* **59**, 2351 (1999).
- [4] O. Hashimoto and H. Tamura, *Prog. Part. Nucl. Phys.* **57**, 564 (2006).
- [5] K. Tanida *et al.*, *Phys. Rev. Lett.* **86**, 1982 (2001).
- [6] K. Hagino and T. Koike, *Phys. Rev. C* **84**, 064325 (2011).
- [7] M. T. Win and K. Hagino, *Phys. Rev. C* **78**, 054311 (2008).
- [8] M. T. Win, K. Hagino, and T. Koike, *Phys. Rev. C* **83**, 014301 (2011).
- [9] J. M. Yao, Z. P. Li, K. Hagino, M. Thi Win, Y. Zhang, and J. Meng, *Nucl. Phys. A* **868**, 12 (2011).
- [10] K. Hagino, J. M. Yao, F. Minato, Z. P. Li, and M. Thi Win, *Nucl. Phys. A* **914**, 151 (2013).
- [11] F. Minato and K. Hagino, [arXiv:1305.2027](https://arxiv.org/abs/1305.2027) [nucl-th].
- [12] F. Minato and K. Hagino, *Phys. Rev. C* **85**, 024316 (2012).
- [13] F. Minato, S. Chiba, and K. Hagino, *Nucl. Phys. A* **831**, 150 (2009); F. Minato and S. Chiba, *ibid.* **856**, 55 (2011).
- [14] M. Isaka, M. Kimura, A. Dote, and A. Ohnishi, *Phys. Rev. C* **83**, 044323 (2011); **83**, 054304 (2011); M. Isaka, H. Homma, M. Kimura, A. Dote, and A. Ohnishi, *ibid.* **85**, 034303 (2012); M. Isaka, M. Kimura, A. Dote, and A. Ohnishi, *ibid.* **87**, 021304 (2013).
- [15] D. Vretenar, W. Pöschl, G. A. Lalazissis, and P. Ring, *Phys. Rev. C* **57**, R1060 (1998).
- [16] X.-R. Zhou, A. Polls, H.-J. Schulze, and I. Vidaña, *Phys. Rev. C* **78**, 054306 (2008).
- [17] I. Tanihata *et al.*, *Phys. Rev. Lett.* **55**, 2676 (1985).
- [18] A. Ozawa *et al.*, *Nucl. Phys. A* **691**, 599 (2001); **693**, 32 (2001).
- [19] I. Tanihata, H. Savajols, and R. Kanungo, *Prog. Part. Nucl. Phys.* **68**, 215 (2013).
- [20] K. Hagino, I. Tanihata, and H. Sagawa, in *100 Years of Subatomic Physics*, edited by E. M. Henley and S. D. Ellis (World Scientific, Singapore, 2013), pp. 231–272.
- [21] M. Takechi *et al.*, *Phys. Lett. B* **707**, 357 (2012).
- [22] R. J. Glauber, in *Lectures in Theoretical Physics*, Vol. I (Interscience, New York, 1959), p. 315.
- [23] G. F. Bertsch, B. A. Brown, and H. Sagawa, *Phys. Rev. C* **39**, 1154 (1989).
- [24] J. Al-Khalili and F. Nunes, *J. Phys. G* **29**, R89 (2003).
- [25] Y. Ogawa, K. Yabana, and Y. Suzuki, *Nucl. Phys. A* **543**, 722 (1992).
- [26] Y. Ogawa, T. Kido, K. Yabana, and Y. Suzuki, *Prog. Theo. Phys. Suppl.* **142**, 157 (2001).
- [27] A. C. Merchant and N. Rowley, *Phys. Lett. B* **150**, 35 (1985).
- [28] B. Buck, A. C. Merchant, and N. Rowley, *Nucl. Phys. A* **327**, 29 (1979).
- [29] S. Sack, L. C. Biedenharn, and G. Breit, *Phys. Rev.* **93**, 321 (1954).
- [30] J. S. Al-Khalili and J. A. Tostevin, *Phys. Rev. Lett.* **76**, 3903 (1996).
- [31] W. Horiuchi, Y. Suzuki, B. Abu-Ibrahim, and A. Kohama, *Phys. Rev. C* **75**, 044607 (2007).
- [32] B. Abu-Ibrahim, W. Horiuchi, A. Kohama, and Y. Suzuki, *Phys. Rev. C* **77**, 034607 (2008).
- [33] J. M. Hauptman, J. A. Kadyk, and G. H. Trilling, *Nucl. Phys. B* **125**, 29 (1977).